REPORT

Measurement of electron depth-dose distribution in water and determination of Linac beam energy

M R McEwen and A J Williams
Centre for Ionising Radiation and Acoustics

JULY 1996

NPL EXTERNAL REPORT CIRA(EXT)011

NPL
National Physical Laboratory

CIRA(EXT)011

July 1996

Measurement of electron depth-dose distributions in water and determination of Linac beam energy

M R McEwen and A J Williams
Centre for Ionising Radiation and Acoustics
National Physical Laboratory
Teddington
Middlesex
United Kingdom
TW11 0LW

ABSTRACT

A system has been developed to accurately measure the practical range of electrons from the NPL Linear Accelerator over the energy range 4-20 MeV. The system uses a linear scanner together with a parallel plate ionization chamber to obtain depth-ionization curves. These are then converted to depth-dose data from which the practical range and other parameters are derived. Range-energy relationships can be used to give a measure of the Linac beam energy. It is estimated that the uncertainty in measuring the practical range at 19 MeV is ±0.45% (at an approximate confidence level of 95%). This uncertainty increases as the energy decreases (to ±1.54% at 4 MeV).

The system has also been used to improve the determination of stopping power ratios by measuring the ratio of ranges for two media, namely water and graphite.

CIRA(EXT)011

ISSN 1361-4053

National Physical Laboratory
Teddington, Middlesex, United Kingdom, TW11 0LW

Approved on behalf of Managing Director, NPL,
by A J Marks, Director, Centre for Ionising Radiation and Acoustics

CONTENTS

TABLES

ILLUSTRATIONS

1 INTRODUCTION

There are various ways of determining the electron beam energy from a linear accelerator (Linac). The most accurate method is to use a calibrated magnetic spectrometer (Wessel et al, 1979), but this technique tends to be rather time consuming and the necessary equipment is not always available. Other methods have been suggested such as detecting Cerenkov radiation in low pressure gases (Almeida and Almond, 1974) and activation analysis (Almond, 1967, Klevenhagen, 1993). Determination of the total charge and energy using a Faraday cup can also be used. A system similar to this has been developed at NPL using a total absorption calorimeter together with a calibrated toroidal charge monitor to determine the electron beam energy (Williams, 1994). However, all these systems tend to be rather complex and a somewhat simpler system is required that can be used for regular checks of the Linac output.

Various techniques can be used for such checks but nearly all rely on the penetration of electrons into a medium. A typical electron depth-dose curve in water is shown in Figure 1. The two most important parameters obtained from such a curve are R_{50}, defined as the depth at 50% of the peak dose; and R_p (the practical range), defined as the point where the extrapolation from the point of maximum gradient on the downward part of the curve meets the extrapolation of the bremsstrahlung background (ICRU 35, 1984). Other parameters can be obtained from a depth-dose curve but these two are the most useful range parameters.

Considerable work has been done to relate these parameters to beam energy. ICRU Report 35 describes a number of range-energy relationships. These, and others, are used in many of the electron dosimetry protocols around the world. Most relate to the measurement of R_{50} and R_p in water.

2 THE NPL SYSTEM

A schematic of the system is shown in Figure 2. It consists of a 30 cm x 30 cm x 30 cm water phantom, the sides of which are 6 mm thick perspex. A hole 15 cm x 15 cm is cut into the front face of this phantom and replaced by a polystyrene sheet 2 mm thick. This reduces the amount of non-water material in the beam. Tests carried out compared various thicknesses of perspex and polystyrene sheet. The aim was to use the thinnest sheet possible without the sheet bulging out too much under the pressure of the water. The initial bulge for the polystyrene sheet was measured to be 0.2 mm (±0.1 mm) but this was found to increase over time (with the water left in the phantom) to between 0.4 mm and 0.6 mm. A similar pattern was observed when the phantom had been left empty for 9 months and then refilled. The polystyrene was attached to the perspex using a propriety epoxy compound (Tensol 70).

It should be noted at this point that the use of particular manufactured items does not imply any kind of endorsement of that item.

A Therados linear scanner (manufactured by Scanditronix) is attached to the top of the water phantom running parallel to the beam axis. This is operated from outside the exposure room using the LSC-1 controller. This is a flexible device that can be operated in three modes:

i) manual - the position is adjusted using a potentiometer,
ii) scan - the position moves at a constant rate (determined by another potentiometer)
iii) external control - the position is determined by an externally applied voltage.

External control (iii) is the favoured mode of operation as it allows the greatest control and greatest flexibility. The external voltage is supplied by a computer controlled DAC. The limited processor speed and memory of the computer are overcome by transferring the data collected to a PC for analysis. A further modification is a control box that allows computer control from within the irradiation room. This box operates via the computer's inbuilt ADCs and makes setting up much easier.

Attached to the linear scanner is a parallel-plate ionization chamber (NACP-02 type). This is attached to a perspex rod which fastens into the holder on the scanner. Measurements have indicated that the holder/rod/chamber system is very rigid.

The LSC-1 controller has an indicator of position in mm (relative) but for greater resolution (as required for these measurements) the position voltage indicator is read by a 6½-digit DMM (under IEEE control from the computer). The scanner has a nominal calibration of 100 mm/V but, for accuracy, a manual calibration was carried out. For this, a ruler was placed on top of the scanner and a pointer attached to the moving holder. It was found that by using a ruler graduated in ½ mm steps, it was possible to estimate the position with an uncertainty less than 0.2 mm. The holder was moved over about 200 mm with measurements taken at a number of points. This calibration was carried out before each set of measurements and the results for the last 4 years are shown in Figure 3. There is no obvious trend and so the mean for all measurements is taken. This gives a value of 99.74 mm/V, very close to the nominal calibration.

In order to make absolute depth measurements, the effective zero must be determined. This depends upon three separate components:

i) the thickness of the front window of the phantom
ii) the effective point of measurement within the chamber - taken to be at the inside front face. The front face consists of 0.1 mm Mylar and 0.5 mm graphite.
iii) the measured position at which the chamber touches the inside face of the phantom window.

The first two are relatively straightforward, requiring only knowledge of the thickness and composition of the relevant materials. The various materials are scaled to water, correcting for density and stopping power.

The overall uncertainty depended initially upon the determination of the third component. Various methods were used to estimate the position at which the chamber touched the window and it was found that it was easier to see if the chamber was tilted slightly away

from the vertical (the holder on the linear scanner allowed such positioning of the chamber). Repeatability was determined to be of the order of 0.15 mm. This is a measure of repeatability at different times and with different operators. However, this method of "slanting" the chamber introduces another component into the zero measurement - the amount of water between the centre of the chamber and the window when the bottom of the chamber is just touching. After using a telescope and video camera it was found that it was just as accurate to make the measurement by eye. This was only possible once the remote control box described above had been constructed.

The procedure to estimate this offset is as follows:

a) move chamber to touch phantom window
b) move chamber away from window until the perceived distance between the chamber and its reflection is twice as big at one side as at the other
c) the offset is then half the distance moved away from the window

The exact value of this offset can vary but is generally of the order of 0.1 - 0.3 mm (therefore the uncertainty is ± 0.1 mm).

The method of moving the chamber until it touches the front window means that it is not necessary to measure the bulge of the tank. The adopted technique automatically takes care of what can be a difficult measurement. The water is removed from the tank each night, so as to ensure repeatability, and the zero measurement is not made until the water has been in the tank for more than half an hour.

Whilst making the measurements as described above, it became apparent that there was a difference between the indicated and actual position of the chamber holder when going in the forward and reverse directions. Direct measurements indicated a difference of 0.3 mm (±0.1 mm) although this may be larger when the chamber is moved at high velocities. Practical range measurements made in both directions have confirmed this value within the uncertainty. In view of this backlash effect, all zero and offset measurements were made with the chamber moving in the same direction (in this case, towards the phantom window).

3 DATA ACQUISITION

The acquisition method is fairly simple. The scanning chamber and monitor chamber are connected to NPL-built electrometers (Sanders, 1989) set to measure charge rate and the outputs from the electrometers are read by the same DVM that reads the linear scanner position. The electron beam is incident upon the phantom throughout the cycle of measurements. The computer program moves the chamber by fixed steps and then measures the chamber/monitor ratio. The step length and number of steps are variable depending on the beam energy and precision required, and time available for the measurement. For the highest precision three measurements of the chamber ratio are taken at each point. Typically a scan takes eight minutes for 300 steps (step length ~ 0.3 mm or less). The data is saved after each run and then transferred to a PC for analysis. It is generally more convenient to collect several scans and then analyse them together. Although this method is rather clumsy in that it uses two different computers, it does mean that maximum use is made of the available Linac beam time.

A doserate of ~ 1 Gy/min is chosen so that there is no need to make any corrections for ion recombination and the field size is defined by a 15 cm x 15 cm lead collimator immediately in front of the water phantom. The SSD can be varied from 0.7 m to greater than 2 m.

A depth-dose curve obtained with this system (at 12 MeV nominal energy) is shown in Figure 4.

4 ANALYSIS

The depth-ionization data is analysed using the mathematics package Mathcad (MathSoft Inc.). Several different methods of analysis have been used. The simplest is to compare the shapes of two depth-ionization curves. This does not give any measure of beam energy but it is remarkably accurate for looking at variations with time. As can be seen from the definitions of R_{50} and R_p, these parameters are derived using only the part of the curve from the peak onwards. By comparing shapes, you can use the whole curve. The build-up portion is especially useful at low energies since the corresponding low range can be difficult to analyse using the techniques described later. The steepness of the build-up and fall-off of the curve makes this a powerful method in monitoring relative changes in energy. Of course, this technique will only work for two curves obtained under identical Linac conditions and experimental geometry.

However, the majority of the work has been put into accurate determinations of R_{50} and R_p since these are the parameters of most interest.

4.1 Conversion from depth-ionization to depth-dose

The system as described above produces a depth-ionization curve. This is a measure of the dose to the air volume of the chamber in a water phantom and is not the depth-dose distribution within the unperturbed water phantom, which is the ultimate goal. Therefore, the depth-ionization curve must be converted to a depth-dose curve. This is done using tabulated stopping powers (ICRU Report 37, 1984) for water and air and estimating the energy at depth to give a correction factor at each point in the phantom. The procedure is as follows:

1. The tabulated stopping power data is used to give a polynomial least-squares fit of the water-air stopping power ratio versus energy:

$$S_{wa} = a_0 + a_1 E + a_2 E^2 + a_3 E^3 + a_4 E^4$$

where S_{wa} is the water-air ratio and E is the electron energy.

2. The tabulated energy versus depth data (IAEA, 1987) is fitted to another polynomial:

$$E_z = E_0[b_0 + b_1\frac{d}{R_p} + b_2(\frac{d}{R_p})^2 + b_3(\frac{d}{R_p})^3 + b_4(\frac{d}{R_p})^4]$$

where E_z is the energy at depth, E_0 is the energy at the phantom surface, d is the depth and R_p is the practical range for electrons of energy E_0 (this value of R_p is estimated from an initial analysis of the depth-ionization curve).

3. For each point on the depth ionization curve the energy at that depth is evaluated and then the stopping power ratio is calculated. This correction is then applied to give the depth-dose curve.

Although the estimated uncertainty in the stopping power ratio is quite large (~1.5%) it is estimated to only effect the determination of the range parameters to the order of 0.1%

4.2 *R_p analysis*

The first method uses a short linear fit (typically 50 points in length) that is moved down the fall-off portion of the curve. This gives an array of values for the gradient and intercept. These are then combined with the bremsstrahlung background to give an array of values for the practical range. It is then a case of selecting the minimum value (where the gradient is a maximum). The advantage of this method is that it is fairly robust, not greatly affected by noise.

The second method fits a high order polynomial (e.g. $a_0+a_0x+a_2x^2+a_3x^3...$) to the fall-off portion of the curve (90% of peak to 10% of peak). The order of the polynomial depends on the shape of the curve but is generally 5th order or greater. This is then differentiated twice to give the point of inflexion, which must, by definition, be the point of maximum gradient. This gradient is then evaluated to give the practical range. The advantage of this method is that the least-square fit routine uses a large proportion of the data, although because of the high order fit it may be susceptible to "spikes" in the data. The two methods tend to be used in parallel with the linear fit being used as a check on the polynomial routine. The two methods generally agree within 0.2%.

4.3 *R_{50} analysis*

The definition of R_{50} as simply the point at 50% dose means that the analysis is fairly simple. First, the curve is smoothed around the peak to give a good estimate of the peak value dose. Two methods are then used to give R_{50}. The first is a linear interpolation routine to give the x-position at 50% of the peak. The second uses the polynomial analysis described above to fit the fall-off portion of the curve and solves the resulting polynomial to give the 50% point. Again, both methods are generally used and compared to give greater confidence in the result. These two methods generally agree within 0.2%.

4.4 Perturbation and the effective point of measurement

Even with the correction from ionization to dose we still do not have the depth-dose distribution in the undisturbed water phantom. The two related effects which need to be taken into account are the chamber perturbation and the effective point of measurement. For a parallel plate chamber it has been assumed that the perturbation effect is small but recent evidence (Klevenhagen, 1991) suggests that there is a sizeable (up to 1%) backscatter effect. Since the NACP chamber is mainly graphite, the measured ionization will be different from that for a water equivalent chamber. Also, the effective point of measurement for a parallel plate chamber is taken to be just inside the front face of the chamber. However, this is only true when the fluence is primarily entering through the front face. At depth in phantom the fluence tends towards an isotropic distribution and in such a situation the point of measurement moves towards the centre of the air volume (2 mm air gap for NACP). As the depth is further increased towards the practical range the fluence will again tend towards being unidirectional, through the front face.

This problem is common to all chamber types. However, since relative measurements over time are of the greatest interest, it is not a significant problem as long as the same chamber type is used for each measurement.

5 UNCERTAINTIES

There are a number of components that contribute to the overall uncertainty in measuring R_{50} and R_p and these are shown in Table 1. There are further uncertainties if one then uses these parameters to obtain the Linac beam energy but this is not really of interest here, since the main aim is to monitor changes in energy.

The overall uncertainty in measuring R_p and R_{50} is estimated (at the 95% confidence level) to be 0.45% for 8-19 MeV, 0.83% for 6 MeV and 1.54 % for 4 MeV. As can be seen from Table 1, the uncertainty at the lowest energies is dominated by the random variation between runs. This is due to the fact that the ranges in water are very small (2 cm for 6 MeV, 1.6 cm for 4 MeV) and the scanner positioning is not accurate enough at very small step lengths. The operation of the NPL Linac is such that any change in output energy should be the same at all electron energies, and consequently there is more to be gained by making measurements at higher energies and inferring the results for the lowest beam energies.

6 RESULTS

Range measurements have been made 5 times in the last 3 years - February 1993, December 1993, January 1994, January 1995 and December 1995. The depth-ionization curves were analysed in the same way each time but there appeared to be large differences between measurements - up to 5%. See Table 2 which shows the original values for R_{50} and R_p.

7 DISCUSSION

The differences as shown in Table 2 are too large to be the result of random variations. The two main possibilities are that there was either some systematic effect not corrected for, or the beam energy was really varying from year to year. This second option was considered since there was some evidence from other measurements that the Linac beam energy had varied at some time in the past. However, the variations over time at different energies were not consistent at anything greater than the 1% level so it was likely that there was some systematic effect that hadn't been taken into account. There are a number of possibilities:

7.1 Real variations in electron energy due to variations in the bending magnetic field

The NPL Linac employs a 270° "Pretzel" bending magnet. This is an achromatic magnet that utilises carefully designed pole-pieces so that although different energy electrons take different trajectories within the varying magnetic field, the electrons emerge from the magnet in the same direction irrespective of energy. Incorporated within the magnet assembly is a pair of tungsten plates which define a slit through which only a certain range of electron energies is transmitted. By using a very narrow slit width and sampling the electron current at different positions within the magnet one can obtain the electron energy spectrum. A typical spectrum is shown in Figure 5. See McEwen (1993) for more detail.

It is possible to vary the mean electron energy by small amounts, typically 0.1-0.2 MeV, by slightly altering the Linac tuning. Depth-ionization measurements were then made to look at the change in practical range with changing electron energy. The measured change was in very good agreement (within 0.1%) with the predicted change from knowledge of the change in mean electron energy.

One drawback of the achromatic magnet (combined with the "tuning" method used on the Linac) is that the magnetic field (determined by the magnet current) determines the transmitted electron energy. Therefore, for accurate depth-ionization measurements, possibly made over days or weeks, it is important that the magnet current remains constant at the 0.1% level, or else the effect of changing current must be taken into account. Without such a correction it is not possible to monitor electron energy changes with time using practical ranges. This is a possible reason for the change in range measurements seen for 1993 to 1995.

An experiment was thus carried out in which the magnet current was deliberately varied (with the same electron energy) and the apparent change in the spectrum measured. From this, a correction was obtained for changes in magnet current. By returning to the original experimental data it was possible to extract the values for the magnet current at each depth-ionization measurement. The range measurements could then be corrected for the real change in energy due to the magnet. A value is chosen arbitrarily as the "standard" setting to which all results are corrected.

7.2 Underestimate of the uncertainties

It was possible that we had underestimated the uncertainties associated with setting the system up each time it was used. For example, the zero measurements described above could be less accurate than we believed. An experiment was therefore carried out to look at such an effect. The procedure was as follows: a) the system was set up; b) depth-ionization curves

were measured for a 10 MeV electron beam; c) the system was dismantled and set up again; d) the depth-ionization measurements were repeated. The results of this experiment were that the practical ranges agreed to within 0.15%, indicating that there we had not underestimated the setting-up uncertainties.

7.3 *Variation due to chamber construction.*

Different chambers had been used to make the measurements at different times. Although they were all NACP-02 type there were two different manufacturers - Scanditronix and Calcam. Investigation of the chambers had already shown that the Calcam chambers were different from the Scanditronix chambers, in terms of polarity and recombination, with the results favouring the Scanditronix chambers. Measurements were therefore carried out in December 1995 to directly compare depth-ionization curves acquired with different chambers on the same system. Bracketed measurements were made to eliminate any effect due to setting-up. The results are shown in Table 3. As can be seen there is a significant difference between the two chambers of approximately 0.3 - 0.4 mm. It is not obvious what can be causing this effect - the simplest solution is a different thickness front window, but it may be more complicated. What can be stated is that the two chamber types are not compatible. Such a difference would have the greatest effect at low energies. The decision one must then make is to choose the manufacturer on which to standardise. In this case the Scanditronix chambers were chosen, for the reasons cited above.

Table 4 shows the range data once corrections had been made for magnet variations and chamber type. Correction is also made for real differences in the electron spectrum. As can be seen, the agreement between the various sets of measurements is much better.

8 BEAM ENERGY DETERMINATION AND COMPARISON WITH OTHER METHODS

By using the range-energy relations described in ICRU Report 35 it is possible to obtain a measure of the electron energy at the phantom surface. This can then be used to obtain a value for the beam energy at the accelerator exit window. Results are shown in Table 5 and can be compared with other methods for determining the Linac beam energy. The range measurements indicate that the actual beam energy is approximately 5% lower than the nominal energy indicated by the Linac.

A system has been developed at NPL to determine the Linac beam energy absolutely. This is described by Williams (1994) and employs a totally absorbing calorimeter combined with a calibrated beam current monitor to measure the total energy and total beam current. From these, the electron energy can be determined. Although this system gives absolute results it is a very time-consuming experiment to perform so is not very good for regular beam energy monitoring. However, by combining this system with range measurements you can circumvent the large uncertainties related to the range-energy relationships. The calorimeter system gives the absolute energy, then the range system monitors any changes on a regular basis. Results from this system give an electron energy 7-8% lower than nominal. The uncertainties are such that it is not possible to say whether the difference between this value and that obtained from the range measurements is significant.

It is also possible to use Monte Carlo simulations of the experimental geometry and match the simulated depth-dose curve to the experimental data by varying the input electron energy. Initial calculations (Ding and Rogers, 1993) indicate agreement with the range measurements at the 1% level. This is within the uncertainties of the comparison. More detailed simulations are currently being carried out at NPL, employing a more realistic electron spectrum and geometry.

9 FURTHER APPLICATIONS

9.1 Determination of stopping power ratios

The system described above has also been used as part of an experiment to determine the stopping power ratio for two media. The technique is described in detail by Burns *et al* (1995), but a brief description is given here. The method relies on measuring the practical range for the same energy electrons in two different media. Initially these two media are water and graphite. By combining these measurements with Monte-Carlo simulations of the experimental geometry it is possible to determine the stopping power ratio water/graphite to a greater accuracy than previously achieved. Initial results indicate that the ratio obtained in this experiment is very close to the ratio obtained from tabulated values (ICRU Report 37).

9.2 Use in X-ray beams

The system, although designed for electron beam work has been used successfully in measuring megavoltage X-ray depth-ionization curves (from ^{60}Co to 19 MV). Various parameters relating to beam quality can then be derived from such curves (e.g. TPR). Alternatively, by rotating the linear scanner through 90° the system can be used to obtain scans of the beam flatness. At NPL this information is required when comparing dosimeters of different dimensions. Unless the beam is completely uniform, a correction is required, for example, when comparing an ionization chamber against the primary standard calorimeter.

10 CONCLUSION

A system has been developed at NPL to accurately measure depth-ionization curves in megavoltage electron and X-ray beams, and to derive important range parameters from these curves. The system is robust and relatively easy to use and shows repeatability over a number of years. It has been used to monitor the Linac beam energy over several years indicating that any energy changes are at the 1% level or below. The system has also been used in an experiment to determine the stopping power ratio, graphite to water, to a greater accuracy than previously obtained.

11 ACKNOWLEDGEMENTS

The authors would like to thank Dr D T Burns for his advice and guidance during the course of this work.

The authors would also like to acknowledge the financial support of the National Measurement Policy Unit of the UK Department of Trade and Industry.

12 REFERENCES

C E Almeida & P R Almond, *Energy calibration of high energy electrons using a cerenkov detector and a comparison with different methods*, Phys. Med. Biol. **19** (1974) 476-483

P R Almond, *The physical measurement of electron beams 6 to 18 MeV, absorbed dose and calibration*, Phys. Med. Biol. **12** (1967) 13-25

D T Burns, S Duane & M R McEwen, *A new method to determine ratios of electron stopping powers to an improved accuracy*, Phys Med Biol **40** (1995) 733-739

G X Ding & D W O Rogers, *Monte Carlo simulation of NPL Linac and calculation of dose distributions and water/air stopping power ratios*, private communication, National Research Council of Canada, 1993.

IAEA, *Absorbed Dose Determination in Photon and Electron Beams*, Technical Report Series No. 277, International Atomic Energy Agency, Vienna, 1987.

ICRU, *Radiation Dosimetry: Electron beams with energies between 1 and 50 MeV*, ICRU Report 35, International Commission on Radiation Units and Measurements, Bethesda, Maryland, 1984.

ICRU, *Stopping Powers for Electrons and Positrons*, ICRU Report 37, International Commission on Radiation Units and Measurements, Bethesda, Maryland, 1984.

S C Klevenhagen, *Implication of electron backscattering for electron dosimetry*, Phys. Med. Biol. **36** (1991) 1013-1018

S C Klevenhagen, *Physics and Dosimetry of Therapy Electron Beams*, Medical Physics Publishing, Wisconsin, 1993.

M R McEwen, *Measurement of the Stopping Power of Graphite*, MSc Thesis, University College London, 1993.

R P Sanders, *The Design and Operation of a High Quality Two-channel Electrometer*, NPL Report RS(INT)106, National Physical Laboratory, Teddington, 1989.

B W Wessel, B R Paliwal, M J Parrot & M C Choi, *Characterization of Clinac-18 electron beam energy using a magnetic analysis method*, Med. Phys **6** (1979) 45-50

A J Williams, *Measurement of the NPL Linear Accelerator Beam Energy by Totally Absorbing Calorimetry*, MSc Thesis, University College London, 1994

Table 1 Summary of uncertainties in measuring R_{50} and R_p (calculated according to NIS 3003[1])

Source	Type A (%) (standard uncertainty)	Type B (%) (standard uncertainty)
Run-to-run variation	0.16% 8-19 MeV 0.3% 6 MeV 0.65 % 4 MeV	
Difference between analysis methods		0.11% 8-19 MeV 0.16% 6 MeV 0.20% 4 MeV
Measurement of zero and slant offset		0.10% 8-19 MeV 0.23% 6 MeV 0.35% 4 MeV
Calibration of scanner		0.03%
Ionization- dose conversion		0.06 %
TOTAL	0.16% 8-19 MeV 0.3% 6 MeV 0.65 % 4 MeV	0.16% 8-19 MeV 0.29% 6 MeV 0.41 % 4 MeV

Overall uncertainty at 95% confidence level (using a coverage factor of k=2):

8-19 MeV	0.45%
6 MeV	0.83%
4 MeV	1.54%

1 NIS 3003, *The expression of uncertainty and confidence in measurement for calibrations*, NAMAS Executive, National Physical Laboratory, Teddington, 1995.

Table 2a Original results of range measurements - R_p (g/cm^2)

Nominal Energy (MeV)	February 1993	December 1993	January 1994	January 1995
4	1.507			1.585
6	2.414			2.486
8	3.313		3.381	3.448
10	4.190			4.232
12	5.072	5.125	5.114	5.162
16	6.862	6.874	6.908	6.939
19	7.884	7.962	7.976	7.993

Table 2b Original results of range measurements - R_{50} (g/cm^2)

Nominal Energy (MeV)	February 1993	December 1993	January 1994	January 1995
4	1.178			1.252
6	1.930			2.053
8	2.725		2.776	2.843
10	3.457			3.508
12	4.221	4.312	4.277	4.278
16	5.759	5.745	5.807	5.812
19	6.657	6.729	6.695	6.747

Table 3 Results of measurements made with two chambers at the same time

Chamber	$R_p(g/cm^2)$	$R_{50}(g/cm^2)$
N37-01 (Scanditronix)	4.245	3.501
C1137 (Calcam)	4.202	3.470
N37-01	4.249	3.505

Table 4a Results when corrected for chamber construction, magnet current and spectrum - R_p (g/cm^2)

Nominal Energy (MeV)	February 1993	December 1993	January 1994	January 1995
4	1.549			1.585
6	2.464			2.486
8	3.413		3.423	3.448
10	4.206			4.232
12	5.099	5.094	5.113	5.162
16	6.932	6.921	6.894	6.939
19	7.934	7.966	7.974	7.993

Table 4b Results when corrected for chamber construction, magnet current and spectrum - R_{50} (g/cm^2)

Nominal Energy (MeV)	February 1993	December 1993	January 1994	January 1995
4	1.218			1.252
6	1.977			2.053
8	2.813		2.811	2.843
10	3.475			3.508
12	4.248	4.286	4.276	4.278
16	5.823	5.784	5.795	5.812
19	6.704	6.732	6.693	6.747

Table 5 Determination of Linac beam energy

Nominal Energy (MeV)	Measured energy (MeV) At accelerator exit window	Measured/Nominal
4	3.79	0.937
6	5.78	0.960
8	7.69	0.962
10	9.39	0.938
12	11.47	0.956
19	18.07	0.947

Overall: Measured/Nominal = 0.950

Figure 1 Schematic of a 16 MeV depth-dose curve showing the two range parameters of interest, R_{50} and R_p (see body of report for full detail)

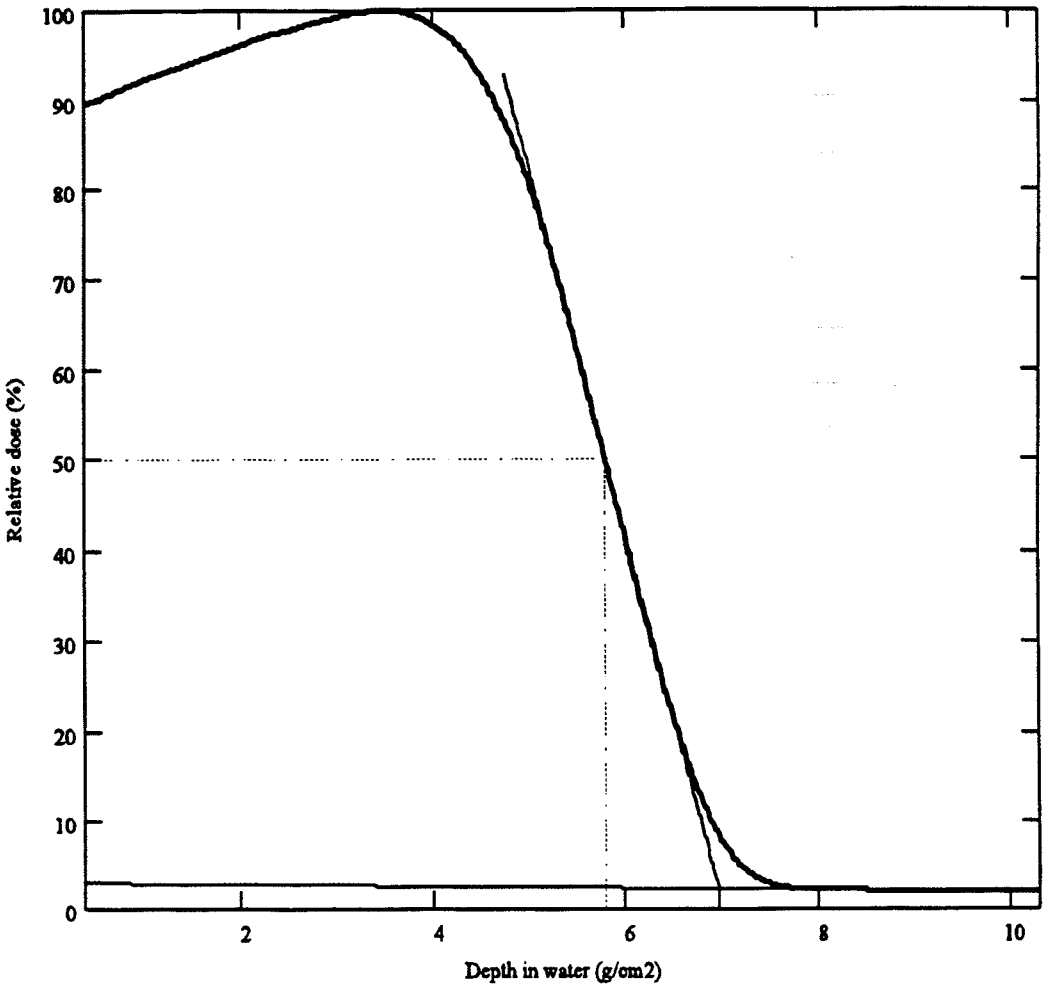

Figure 2 Schematic of apparatus used to acquire depth-ionization curves in water

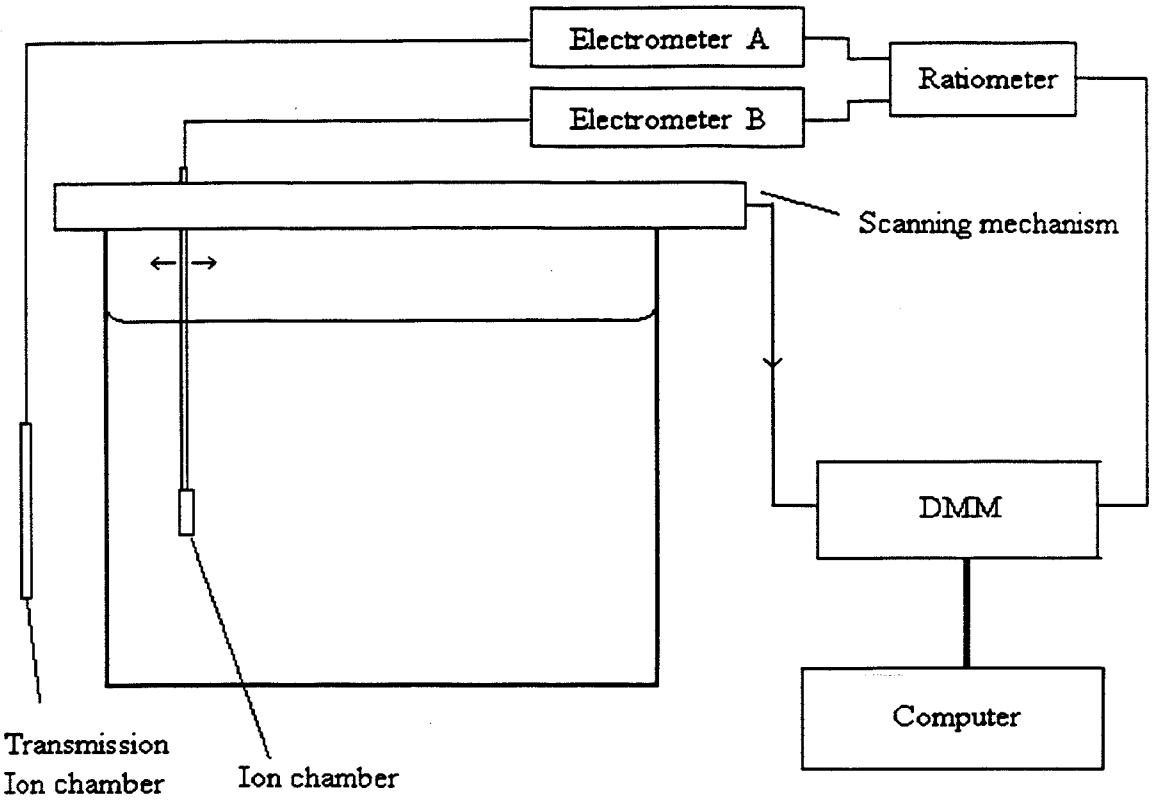

Figure 3 Calibration of the LSC-1 Scan controller

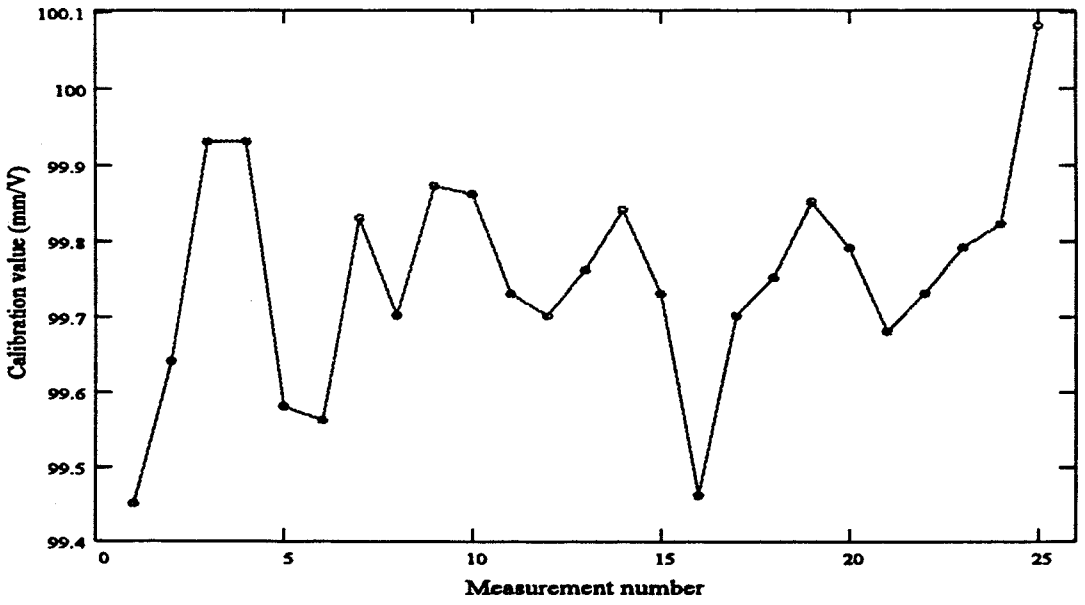

Figure 4 12 MeV depth dose curve

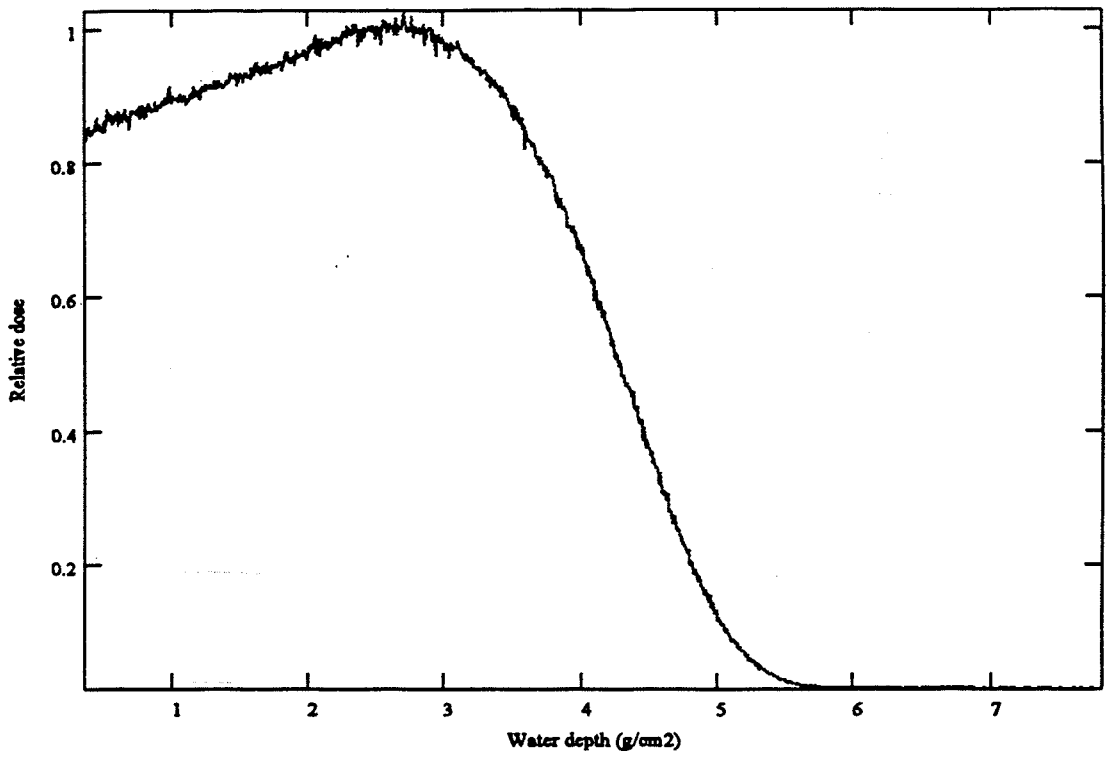

Figure 5 Typical spectrum from NPL Linac